



Published in final edited form as:

*Nat Struct Mol Biol.* 2013 June ; 20(6): 735–739. doi:10.1038/nsmb.2572.

## Structural basis for the recruitment of the human CCR4–NOT deadenylase complex by Tristetraprolin

Marc R. Fabian<sup>1,2,5</sup>, Philipp Frank<sup>3,5</sup>, Christopher Rouya<sup>3,5</sup>, Nadeem Siddiqui<sup>3</sup>, Wi S. Lai<sup>4</sup>, Alexey Karetnikov<sup>3</sup>, Perry J. Blackshear<sup>4</sup>, Bhushan Nagar<sup>3</sup>, and Nahum Sonenberg<sup>3</sup>

<sup>1</sup>Lady Davis Institute for Medical Research, SMBD-Jewish General Hospital. Montréal, Quebec, Canada

<sup>2</sup>Department of Oncology, McGill University, Montreal, Quebec, Canada

<sup>3</sup>Department of Biochemistry and Goodman Cancer Centre, McGill University, Montreal, Quebec, Canada

<sup>4</sup>Laboratory of Signal Transduction, National Institute of Environmental Health Science, NC, USA

### Abstract

Tristetraprolin (TTP) is an RNA binding protein that controls the inflammatory response by limiting the expression of several proinflammatory cytokines. TTP post-transcriptionally represses gene expression by interacting with AU-rich elements (AREs) in 3'UTRs of target mRNAs and subsequently engenders their deadenylation and decay. TTP accomplishes these tasks, at least in part, by recruiting the multi subunit CCR4–NOT deadenylase complex to the mRNA. Here we identify an evolutionarily conserved C-terminal motif in human TTP that directly binds to a central domain of CNOT1, a core subunit of the CCR4–NOT complex. A high-resolution crystal structure of the TTP-CNOT1 complex was determined, providing the first structural insight into an ARE-binding protein bound to the CCR4–NOT complex. Mutations at the CNOT1-TTP interface impair TTP-mediated deadenylation, demonstrating the significance of this interaction in TTP-mediated gene silencing.

### Introduction

Mammalian gene expression is tightly regulated by an array of post-transcriptional control programs, including mRNA translation and stability. The mRNA 3' untranslated region (UTR) plays a critical role in post-transcriptional control via *cis*-acting elements, such as

Corresponding authors: Marc Fabian (marc.fabian@mcgill.ca), Bhushan Nagar (bhushan.nagar@mcgill.ca), Nahum Sonenberg (nahum.sonenberg@mcgill.ca).

<sup>2</sup>These authors contributed equally to this work

#### ACCESSION CODES

Structure factors and coordinates for the TTP-CNOT1 complex have been deposited in the Protein Data Bank with accession the code 4J8S.

#### AUTHOR CONTRIBUTIONS

M.R.F., F.F., C.R. and N. Siddiqui designed experiments. M.R.F. and C.R. performed binding assays and *in vitro* deadenylation assays. N. Siddiqui performed ITC experiments. F.F. crystallized the CNOT1-TTP complex and B.N. and F.F. determined its structure. W.S.L. and P.J.B. performed *in vivo* stability assays. A.K. provided technical support. M.R.F., F.F., B.N. and N.S. wrote the manuscript.

micro (mi)RNA target sites and adenylate uridylate-rich elements (AREs)<sup>1,2</sup>. These RNA elements are targeted by miRNAs and ARE-binding proteins (ARE-BPs). Tristetraprolin (TTP) is an ARE-BP, which represents the prototypical member of the TIS11 [TPA (12-O-tetradecanoylphorbol-13-acetate) inducible sequence-11] family of RNA-binding proteins that include the TTP-related proteins butyrate response factors (BRF)-1 and -2<sup>3-5</sup>. TTP is an important regulator of the inflammatory response, and a *bona fide* tumor suppressor in lymphomas<sup>6-9</sup>. TTP, along with BRF-1 and BRF-2, bind to AREs in the 3'UTRs of target mRNAs through their tandem zinc finger domains<sup>10</sup>, to promote mRNA deadenylation and subsequent decay by recruiting the CCR4–NOT complex<sup>11</sup>. The N-terminal and C-terminal domains of TTP effect deadenylation through the CCR4–NOT complex<sup>11,12</sup>. However, controversy exists with respect to how TTP interacts with the deadenylase machinery. One report concluded that components of the CCR4–NOT complex interact only with the TTP N-terminal domain<sup>11</sup>, whereas another only documented interactions with the TTP C-terminal domain<sup>12</sup>. Thus, it is currently unclear how TTP physically interacts with the CCR4–NOT complex to bring about deadenylation.

CCR4–NOT is a multi-subunit protein complex originally described in *Saccharomyces cerevisiae* as a global regulator of transcription and the cell cycle<sup>13</sup>. However, it has since gained prominence as a master regulator of mRNA stability that interfaces with several key post-transcriptional control programs, including those mediated by miRNAs and by TTP family proteins<sup>14</sup>. The mammalian CCR4–NOT complex is comprised of multiple proteins, termed **CCR4–NOT** (CNOT) subunits. The CNOT1 subunit acts as a scaffold for other CCR4–NOT components, including the CNOT6 (CCR4) and CNOT7 (CAF1) deadenylases. In this study, we have identified a novel motif in TTP that binds CNOT1, elucidated the structural basis for this interaction, and established its significance for TTP-mediated gene silencing.

## Results

### TTP directly binds CNOT1

The human CNOT1 subunit is a large scaffolding protein that associates with TTP through unknown contacts<sup>12</sup>. To demonstrate that CNOT1 directly interacts with TTP, as recently postulated<sup>12</sup>, we performed *in vitro* co-precipitation experiments using recombinant MBP-fused TTP (Fig. 1A), and a series of GST-fused CNOT1 fragments covering the entire CNOT1 isoform C (2371 aa) protein (Fig. 1B). A CNOT1 fragment encompassing residues 727–1266 efficiently bound MBP–TTP, whereas all other CNOT1 fragments did not (Supplementary Fig. 1). We subsequently mapped the region of CNOT1 that binds TTP to residues 800–1015 (Fig. 1C and Supplementary Fig. 1).

Next, we set out to identify what region of TTP binds to the CNOT1<sub>800–1015</sub> fragment. To this end, we generated MBP-fused TTP fragments containing either the TTP N-terminal (residues 1–99) or C-terminal (residues 174–326) regions (Fig. 1A), which have been reported to associate with the CCR4–NOT<sup>11,12</sup>. GST-CNOT1<sub>800–1015</sub> did not interact with the TTP N-terminal domain in binding assays (Fig. 1C). In contrast, it bound the TTP C-terminal domain very efficiently (~50% of input) (Fig. 1C). Sequence alignment of the TTP C-terminal domain (CTD) and its related proteins, BRF-1 and BRF-2, revealed two

conserved patches of amino acids in the TTP CTD: residues 179–192 and 314–326 (Supplementary Fig. 2). GST–CNOT1<sub>800–1015</sub> bound MBP–TTP lacking amino acids 179–192 [(TTP–MUT1) Figs. 1A and C]. However, MBP–TTP lacking the terminal 13 amino acids (TTP–MUT2) failed to bind GST–CNOT1<sub>800–1015</sub> (Figs. 1A and C). Importantly, the TTP C-terminal amino acid sequence is highly conserved in Tis11 homologs, including in *Xenopus tropicalis*, *Drosophila melanogaster* and *Caenorhabditis elegans* (Fig. 1D). Taken together, these results demonstrate that CNOT1 interacts with an evolutionarily conserved amino acid motif at the C-terminus of TTP.

### Structural determination of the TTP–CNOT1 interaction

To gain structural insight into the CNOT1–TTP interaction we solved the crystal structure of a TTP-interacting fragment of CNOT1 (residues 800–999) in complex with a peptide covering residues Ala312 to Glu326 of hTTP (Fig. 1D) at 1.5 Å resolution (Fig. 2A and Table 1). The N-terminal 20 residues (800–819) of the CNOT1 fragment are disordered, whereas TTP could be modeled from residues Arg314 to Ser325. CNOT1<sub>820–999</sub> consists of eight  $\alpha$ -helices stacked as a series of helix-turn-helix motifs in an arrangement similar to the HEAT repeats of the **M**iddle domain of **I**nitiation **F**actor **4G** (MIF4G)<sup>15</sup> (Supplementary Fig. S3A). The MIF4G domain is generally utilized as a protein-protein interaction domain and is found in numerous scaffolding proteins involved in the regulation of translation and RNA metabolism<sup>16</sup>. The main difference between the CNOT1 domain and the MIF4G domain resides at the N-terminal region, where the MIF4G domain forms the first HEAT repeat. In CNOT1, this region forms a long loop held in place by Trp828, which folds over  $\alpha$ 3 and contributes to a highly acidic surface adjacent to the TTP binding site (not shown in figure).

The TTP binding site is located close to the N-terminus of CNOT1<sub>820–999</sub>, and is formed by a highly conserved hydrophobic groove between helices  $\alpha$ 1 and  $\alpha$ 3 that is flanked by negatively charged patches of amino acids (Fig. 2B). The central portion of the TTP peptide forms a short, two-turn amphipathic  $\alpha$ -helix resulting in the insertion of Leu316, Ile318, Phe319, and Ile322 into the hydrophobic groove of CNOT1 (Fig. 3A). The bottom of the groove is lined with aromatic residues Phe847, Tyr851, and Tyr900 (Fig. 3B). A network of electrostatic interactions between several polar residues located at the termini of the TTP peptide and the surrounding negatively charged residues in CNOT1 is also formed. The most prominent of these interactions is a salt bridge between Glu893 of CNOT1 and Arg315 of TTP at the edge of the groove (Fig. 3B). Hydrogen bonding between Glu893 and Tyr900 of CNOT1 with residues Arg315 and Ser323 of TTP, respectively, generates a stable closed-loop conformation in the TTP peptide (Fig. 3B). Additional contacts stabilizing the complex are provided by hydrogen bonds on the solvent exposed side of the TTP helix between residues Pro317 and Arg321 of TTP with Asn844 and Gln848 of CNOT1, respectively (Fig. 3B). The sum of these interactions confers an affinity ( $K_d$ ) of  $\sim 2\mu\text{M}$  between the TTP peptide and CNOT1<sub>820–999</sub> as measured by isothermal titration calorimetry (ITC) experiments (Supplementary Fig. S3B).

We generated mutants of TTP to biochemically validate the structure. Alanine substitutions of Arg315, which makes a salt bridge with Glu893 of CNOT1, and Phe319, which is at the

center of the hydrophobic interaction site and forms Van der Waals contacts with the CNOT1 surface (Supplementary Fig. 4A), in the TTP-CTD abolished its interaction with CNOT1<sub>800–1015</sub> *in vitro* (Fig. 3C). In addition, mutating Phe319 to alanine in the TTP peptide disrupted its binding to CNOT1<sub>820–999</sub> [K<sub>d</sub> = ~7mM (Supplementary Fig. S3C)]. Mutation of Asn320, which does not make contact with CNOT1, to alanine failed to disrupt the TTP-CNOT1 interaction (Fig. 3C). Taken together, these data demonstrate that the TTP-CNOT1 interaction requires several invariant residues in the C-terminus of TTP, a sequence we now refer to as a TTP-CCR4-NOT-Interaction Motif (TTP-CIM).

### TTP-CNOT1 contact promotes mRNA deadenylation *in vitro*

TTP requires its CTD to effect maximal deadenylation of target mRNAs<sup>11,12</sup>. To examine the functional significance of the interaction between CNOT1 and TTP, we established an *in vitro* assay for TTP-mediated deadenylation. Using the λN-BoxB system<sup>17</sup>, we artificially tethered recombinant TTP proteins to an RNA reporter containing 5 BoxB stem-loops and a 98-nucleotide poly(A) tail (5-BoxB-pA), which was added to a cell-free extract derived from mouse Krebs-2 ascites (termed Krebs extract) (Fig. 4A). This strategy has been used successfully to biochemically dissect the mechanics of miRNA-mediated deadenylation by the CCR4-NOT complex<sup>18</sup>. Recombinant wild-type GST-TTP was unable to mediate deadenylation, whereas wild-type GST-λNHA-TTP engendered complete deadenylation of 5-BoxB-pA RNA in the Krebs extract within 2 hours (Fig. 4B). In contrast, a TTP mutant that could not bind to CNOT1 (TTP-Phe319Ala) displayed severely impaired deadenylation, with deadenylation barely detectable by 2 h (Fig. 4B, right panel). Similar results were obtained when using a polyadenylated reporter containing two TTP-binding sites derived from the tumor necrosis factor 3'UTR (TNF-ARE-pA), a *bona fide* TTP mRNA target (Fig. 4C). Wild-type GST-TTP engendered complete deadenylation of TNF-ARE-pA by 2 hours, whereas GST-TTP-Phe319Ala displayed partial and incomplete deadenylation (Fig. 4D). Taken together, these results demonstrate that TTP-mediated deadenylation *in vitro* requires the TTP-CTD-CNOT1 interaction, irrespective of whether TTP is directly binding or being artificially tethered to a target RNA.

### TTP-CNOT1 contact promotes mRNA decay *in vivo*

We also examined the significance of the TTP-CNOT1 interaction on the stability of a TTP-targeted reporter mRNA *in vivo*. We employed a plasmid containing the mouse MARCKS-like protein (MLP) promoter and coding region that is fused to the TTP-targeted TNFα 3'UTR (MLP-TNF3'), which has previously served as a reporter to assay TTP function in cell cultures<sup>19</sup>. HEK-293 cells were co-transfected with the MLP-TNF3' reporter plasmid, along with a plasmid coding for (i) green fluorescent protein (GFP), (ii) wild-type TTP or (iii) various TTP mutants (Figs. 4E and F). We observed significantly less MLP-TNF3' RNA in wild-type TTP-expressing cells as compared to GFP-expressing cells, indicative of an increase in reporter mRNA degradation. Similar effects on MLP-TNF3' RNA stability were observed in cells expressing a TTP mutant that contains the TTP-CIM but lacks four C-terminal amino acids (1–322) (lane 4). In contrast, MLP-TNF3' RNA was significantly stabilized in cells expressing a TTP mutant where an additional 9 amino acids have been deleted, thereby removing the TTP-CIM (1–313) (lane 5). Thus, these results strongly

suggest that TTP requires its C-terminal CNOT1-interacting motif to bring about efficient decay of a target mRNA *in vivo*.

## Discussion

We have identified a novel CCR4–NOT-interaction motif (CIM) at the C-terminus of human TTP. The TTP-CIM directly binds the CNOT1 subunit of the CCR4–NOT complex. Importantly, this represents the first structure of the interface between an ARE-BP and the CCR4–NOT complex. Furthermore, our data demonstrate that optimal TTP-mediated deadenylation requires the TTP-CIM to be bound to CNOT1, as disrupting this interaction impairs, but does not completely abolish, deadenylation *in vitro* (Figs. 4A and B) and mRNA decay *in vivo* (Fig. 4C). These data fit well with previous studies demonstrating that the TTP N-terminal domain facilitated deadenylation of target mRNAs in a CCR4–NOT complex-dependent manner. How the deadenylase machinery interacts with the TTP N-terminal domain remains to be determined. Interestingly, the TTP-binding domain of CNOT1 is N-terminally adjacent to the CNOT1 domain that binds the CAF1 deadenylase<sup>20,21</sup>. It is therefore plausible that TTP binding next to CAF1 on CNOT1 may help position the CAF1 deadenylase such that it has unimpeded access to the mRNA poly(A) tail (Fig. 4G).

TTP residues that interact with CNOT1 are phylogenetically conserved in Tis11 proteins, including the *Drosophila melanogaster* Tis11 homolog and the *Caenorhabditis elegans* protein CCCH-1 (Fig. 1D). Moreover, CNOT1 residues that form a groove, which contains amino acids that interact with the TTP-CIM (Phe847, Tyr851, Glu893 and Tyr900) are highly conserved across these species as well (Supplementary Fig. 4B). A recent study reported the crystal structure of the yeast Not1 N-terminal region (residues 154–753)<sup>20</sup>. It consists of 13 HEAT repeats, of which repeats 10–13 (residues 571–746) correspond to the 4 HEAT repeats found in human CNOT1<sub>820–999</sub>. Although yeast Not1 and human CNOT1 proteins share only 35% sequence identity in this region, the structures are very similar with a *C $\alpha$* -RMSD of 1.19 Å (Supplementary Figs. 4C and D). Interestingly, yeast Not1 HEAT repeats 10–13 form a separate unit within the protein in that they are arranged in a parallel fashion while there is a rotation by 90° with respect to repeats 1–9<sup>20</sup>. This suggests that HEAT repeats 10–13 form a separate domain. Our results confirm this notion since we show that this domain is stable and can carry out its function of TTP recruitment in the absence of the more N-terminal HEAT repeats. The residues in human CNOT1 that form the TTP docking site are also conserved in yeast Not1, suggesting that they may also act as a protein binding site. However, the yeast Tis11 homolog CTH1 (Cysteine **T**hree **H**istidine 1) does not contain a sequence that shares any detectable homology to the hTTP-CIM. Nevertheless, it is conceivable that ancient NOT1 proteins maintained this protein-interaction groove, which was exploited during the course of eukaryotic evolution by proteins such as TTP. CNOT1 binds the miRNA-associated GW182 protein through two conserved CIMs and additional tryptophan-containing sequences<sup>18,22</sup>. However, the TTP-CIM does not share homology with the GW182 CIMs, suggesting that TTP and GW182 bind to different regions of CNOT1.

Mouse TTP activity is controlled by phosphorylation on a number of residues, including Ser52 and Ser178 (Ser60 and Ser186 in human TTP, respectively) by the p38 MAPK-activated protein kinase 2 (MK2)<sup>23</sup>. Serines 52 and 178, when phosphorylated, act as substrates for 14-3-3 adaptor proteins that bind to and stabilize TTP<sup>23,24</sup>. Phosphorylation of TTP via MK2 also impairs TTP recruitment of the CCR4–NOT complex and TTP-mediated deadenylation<sup>25,26</sup>. Based on these data, it has been postulated that 14-3-3 binding to TTP impairs deadenylase recruitment<sup>26</sup>. However, our data demonstrate that 14-3-3 binding sites (Ser52 and Ser178) do not overlap with the C-terminal TTP CIM. Notwithstanding these data, MK2-induced TTP phosphorylation partially inhibits CCR4–NOT association even when these serines are mutated in tandem to alanines, thereby abolishing 14-3-3 binding<sup>26</sup>. It has therefore been suggested that additional phosphorylation sites act to inhibit deadenylase recruitment to TTP<sup>26</sup>. Interestingly, MK2 has also been reported to phosphorylate TTP and BRF-1 on a highly conserved serine residue residing within the TTP-CIM [Ser323 in hTTP (Fig. 1D)]<sup>23</sup>. Our structural data indicate that Ser323 forms multiple contacts at the TTP–CNOT1 interface, both within the TTP peptide and with CNOT1 (Fig 3B). Thus, the addition of a phosphate group to Ser323 would likely perturb TTP–CNOT1 binding. Indeed, a TTP-CIM peptide containing a phospho-Ser323 binds with a significantly lower affinity to CNOT1<sub>820–999</sub> [ $K_d = \sim 625\mu\text{M}$  (Supplementary Fig. S3D)] as compared to wild-type. Taken together, these data suggest that the ability of the TTP-CIM to bind CNOT1 is regulated through the p38-signaling pathway. This model may help explain how MK2-phosphorylation regulates TTP recruitment of the CCR4–NOT complex. It is possible that 14-3-3 proteins and the CCR4–NOT complex compete for TTP binding. Phosphorylation of Ser323 may therefore aid the TTP transition from being bound to the CCR4–NOT complex to interacting with 14-3-3 proteins. Whether this post-translational modification plays a role in regulating TTP-mediated silencing, however, remains to be determined.

## Supplementary Material

Refer to Web version on PubMed Central for supplementary material.

## Acknowledgments

This work was supported by Canadian Institutes of Health Research grants to N.S. (MOP-93607) and to B.N. (MOP-82929). N.S. was also supported by a Howard Hughes Medical Institute (HHMI) Senior International Scholarship. P.B. was supported by the Intramural Research Program of the US National Institutes of Health, National Institute of Environmental Health Sciences. N. Siddiqui holds a fellowship from the Cole Foundation.

## References

1. Fabian MR, Sonenberg N, Filipowicz W. Regulation of mRNA translation and stability by microRNAs. *Annual review of biochemistry*. 2010; 79:351–79.
2. von Roretz C, Di Marco S, Mazroui R, Gallouzi IE. Turnover of AU-rich-containing mRNAs during stress: a matter of survival. *Wiley interdisciplinary reviews. RNA*. 2011; 2:336–47. [PubMed: 21957021]
3. Sanduja S, Blanco FF, Dixon DA. The roles of TTP and BRF proteins in regulated mRNA decay. *Wiley interdisciplinary reviews. RNA*. 2011; 2:42–57. [PubMed: 21278925]
4. Blackshear PJ. Tristetraprolin and other CCCH tandem zinc-finger proteins in the regulation of mRNA turnover. *Biochem Soc Trans*. 2002; 30:945–52. [PubMed: 12440952]

5. Lai WS, Stumpo DJ, Blackshear PJ. Rapid insulin-stimulated accumulation of an mRNA encoding a proline-rich protein. *The Journal of biological chemistry*. 1990; 265:16556–63. [PubMed: 2204625]
6. Sanduja S, Blanco FF, Young LE, Kaza V, Dixon DA. The role of tristetraprolin in cancer and inflammation. *Frontiers in bioscience : a journal and virtual library*. 2012; 17:174–88.
7. Rounbehler RJ, et al. Tristetraprolin impairs myc-induced lymphoma and abolishes the malignant state. *Cell*. 2012; 150:563–74. [PubMed: 22863009]
8. Carballo E, Lai WS, Blackshear PJ. Feedback inhibition of macrophage tumor necrosis factor- $\alpha$  production by tristetraprolin. *Science*. 1998; 281:1001–5. [PubMed: 9703499]
9. Taylor GA, et al. A pathogenetic role for TNF  $\alpha$  in the syndrome of cachexia, arthritis, and autoimmunity resulting from tristetraprolin (TTP) deficiency. *Immunity*. 1996; 4:445–54. [PubMed: 8630730]
10. Lai WS, Carballo E, Thorn JM, Kennington EA, Blackshear PJ. Interactions of CCCH zinc finger proteins with mRNA. Binding of tristetraprolin-related zinc finger proteins to Au-rich elements and destabilization of mRNA. *The Journal of biological chemistry*. 2000; 275:17827–37. [PubMed: 10751406]
11. Lykke-Andersen J, Wagner E. Recruitment and activation of mRNA decay enzymes by two ARE-mediated decay activation domains in the proteins TTP and BRF-1. *Genes & development*. 2005; 19:351–61. [PubMed: 15687258]
12. Sandler H, Kreth J, Timmers HT, Stoecklin G. Not1 mediates recruitment of the deadenylase Caf1 to mRNAs targeted for degradation by tristetraprolin. *Nucleic acids research*. 2011; 39:4373–86. [PubMed: 21278420]
13. Collart MA, Panasenko OO. The Ccr4–not complex. *Gene*. 2012; 492:42–53. [PubMed: 22027279]
14. Goldstrohm AC, Wickens M. Multifunctional deadenylase complexes diversify mRNA control. *Nature reviews. Molecular cell biology*. 2008; 9:337–44.
15. Schutz P, et al. Crystal structure of the yeast eIF4A-eIF4G complex: an RNA-helicase controlled by protein-protein interactions. *Proceedings of the National Academy of Sciences of the United States of America*. 2008; 105:9564–9. [PubMed: 18606994]
16. Ponting CP. Novel eIF4G domain homologues linking mRNA translation with nonsense-mediated mRNA decay. *Trends Biochem Sci*. 2000; 25:423–6. [PubMed: 10973054]
17. Baron-Benhamou J, Gehring NH, Kulozik AE, Hentze MW. Using the lambdaN peptide to tether proteins to RNAs. *Methods in molecular biology*. 2004; 257:135–54. [PubMed: 14770003]
18. Fabian MR, et al. miRNA-mediated deadenylation is orchestrated by GW182 through two conserved motifs that interact with CCR4–NOT. *Nature structural & molecular biology*. 2011; 18:1211–7.
19. Blackshear PJ, et al. Zfp3613, a rodent X chromosome gene encoding a placenta-specific member of the Tristetraprolin family of CCCH tandem zinc finger proteins. *Biol Reprod*. 2005; 73:297–307. [PubMed: 15814898]
20. Basquin J, et al. Architecture of the Nuclease Module of the Yeast CCR4–NOT Complex: the Not1-Caf1-Ccr4 Interaction. *Molecular cell*. 2012
21. Petit AP, et al. The structural basis for the interaction between the CAF1 nuclease and the NOT1 scaffold of the human CCR4–NOT deadenylase complex. *Nucleic acids research*. 2012
22. Chekulaeva M, et al. miRNA repression involves GW182-mediated recruitment of CCR4–NOT through conserved W-containing motifs. *Nature structural & molecular biology*. 2011; 18:1218–26.
23. Chrestensen CA, et al. MAPKAP kinase 2 phosphorylates tristetraprolin on in vivo sites including Ser178, a site required for 14-3-3 binding. *The Journal of biological chemistry*. 2004; 279:10176–84. [PubMed: 14688255]
24. Stoecklin G, et al. MK2-induced tristetraprolin:14-3-3 complexes prevent stress granule association and ARE-mRNA decay. *The EMBO journal*. 2004; 23:1313–24. [PubMed: 15014438]
25. Marchese FP, et al. MAPKAP kinase 2 blocks tristetraprolin-directed mRNA decay by inhibiting CAF1 deadenylase recruitment. *The Journal of biological chemistry*. 2010; 285:27590–600. [PubMed: 20595389]

26. Clement SL, Scheckel C, Stoecklin G, Lykke-Andersen J. Phosphorylation of tristetraprolin by MK2 impairs AU-rich element mRNA decay by preventing deadenylase recruitment. *Molecular and cellular biology*. 2011; 31:256–66. [PubMed: 21078877]
27. Nguyen MN, Tan KP, Madhusudhan MS. CLICK–topology-independent comparison of biomolecular 3D structures. *Nucleic acids research*. 2011; 39:W24–8. [PubMed: 21602266]

Author Manuscript

Author Manuscript

Author Manuscript

Author Manuscript



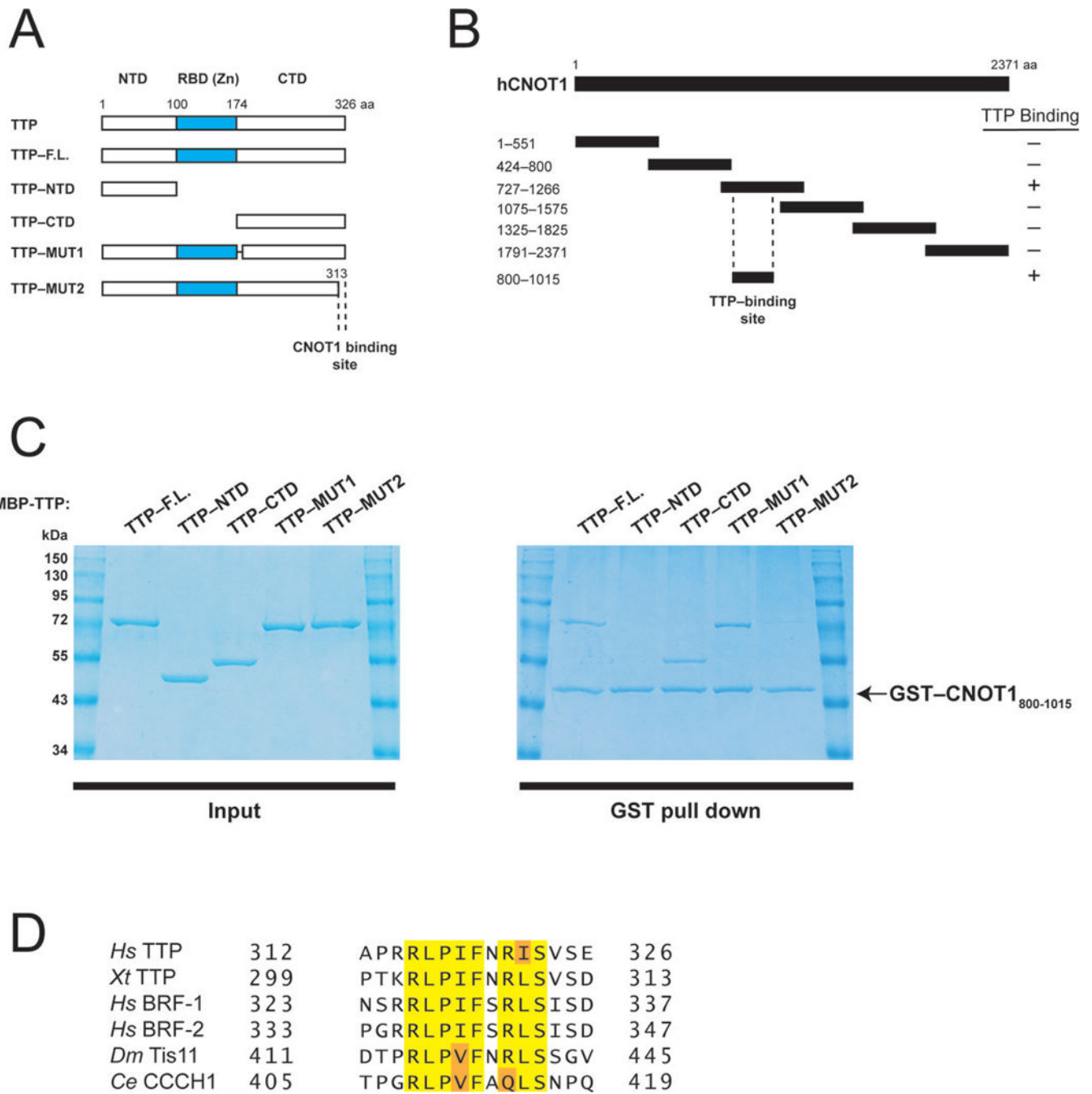


**Figure 1.** Human TTP directly binds a central fragment of CNOT1. (A) Schematic diagram of full-length TTP and TTP fragments used in co-precipitation experiments (Fig. 1C). Dashed lines indicate the region required for CNOT1 binding (Fig. 1C). (B) Schematic diagram of full-length CNOT1 and CNOT1 fragments used in co-precipitation experiments (Fig. 1C and Supplemental Fig. 1). Coordinates are marked to the left of each fragment. Dashed lines indicate the region required for TTP binding (Figure 1C). (C) Right panel: Recombinant glutathione-S-transferase (GST)-tagged CNOT1<sub>800-1015</sub> (Figure 1B) was immobilized on

glutathione-Sepharose beads and incubated with (MBP)-tagged full-length TTP, or TTP fragments (see left panel). Precipitated proteins were separated by SDS-PAGE and visualized by Coomassie staining. **(D)** Sequence alignment of conserved amino acids within the TTP C-terminus that binds CNOT1 of human (*Hs*) TTP, BRF-1, and BRF-2, *Xenopus tropicalis* (*Xt*) TTP, *Drosophila melanogaster* (*Dm*), Tis11 and *Caenorhabditis elegans* (*Ce*) CCCH1. Highlighted are amino acids identical in 100% of proteins (yellow) or conservative substitutions by related amino acids (orange).

Author Manuscript

Author Manuscript

Author Manuscript

Author Manuscript

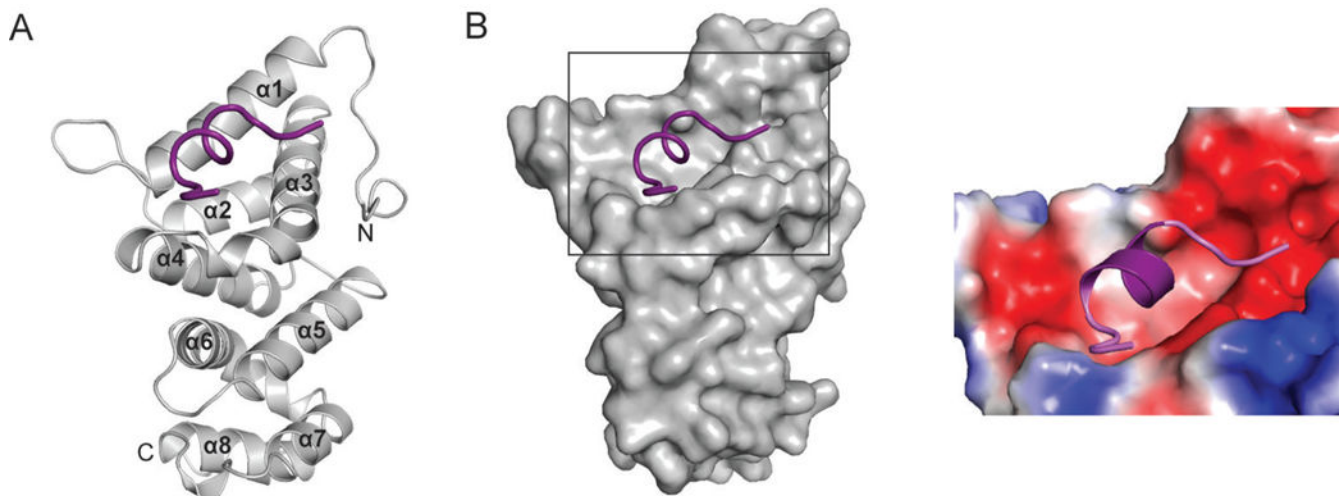


**Figure 2.**

Crystal structure of the TTP-CNOT1 complex. **(A)** Cartoon representation of the crystal structure of human CNOT1<sub>820-999</sub> (grey) in complex with TTP peptide (purple). The eight CNOT1 helices are numbered starting from the N-terminus. **(B)** Left panel: Surface representation of CNOT1<sub>820-999</sub>. The bound TTP<sub>312-326</sub> peptide (purple) is shown as a cartoon representation. Right panel: magnification of TTP binding site on CNOT1<sub>820-999</sub> colored according to electrostatic potential, from dark red ( $-kT/e$ ) to white ( $0 kT/e$ ) to dark blue ( $+5 kT/e$ ).

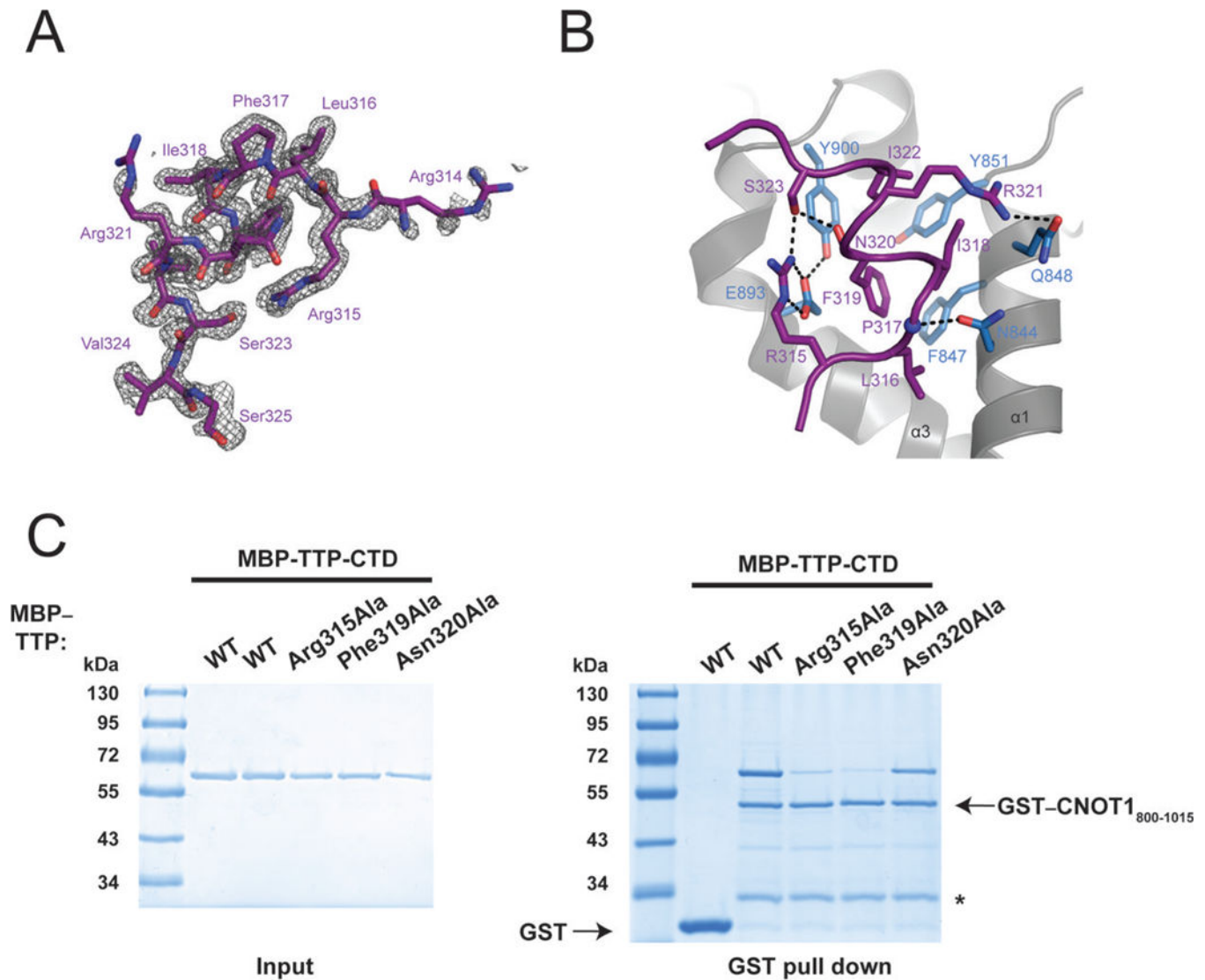


**Figure 3.** Analysis of TTP-CNOT1 interaction. **(A)** Electron density (grey) of the TTP<sub>312-326</sub> peptide (shown as purple sticks). Density ( $F_o - F_c$  of a map calculated by omitting the TTP peptide) is contoured at  $2.5\sigma$ . **(B)** A view of the interface between the CNOT1 domain (grey) and TTP peptide (purple). Interacting side chains of CNOT1 (blue) and TTP (purple) are shown as sticks. The backbone amide of P317 is shown as a blue sphere. Dashed lines indicate hydrogen-bonding interactions. **(C)** Recombinant glutathione-S-transferase (GST)-tagged CNOT1<sub>800-1015</sub> (Figure 1B) was immobilized on glutathione-Sepharose beads and incubated with (MBP)-tagged TTP-CTD, or TTP-CTD mutants. Precipitated proteins were separated by SDS-PAGE and visualized by Coomassie staining.

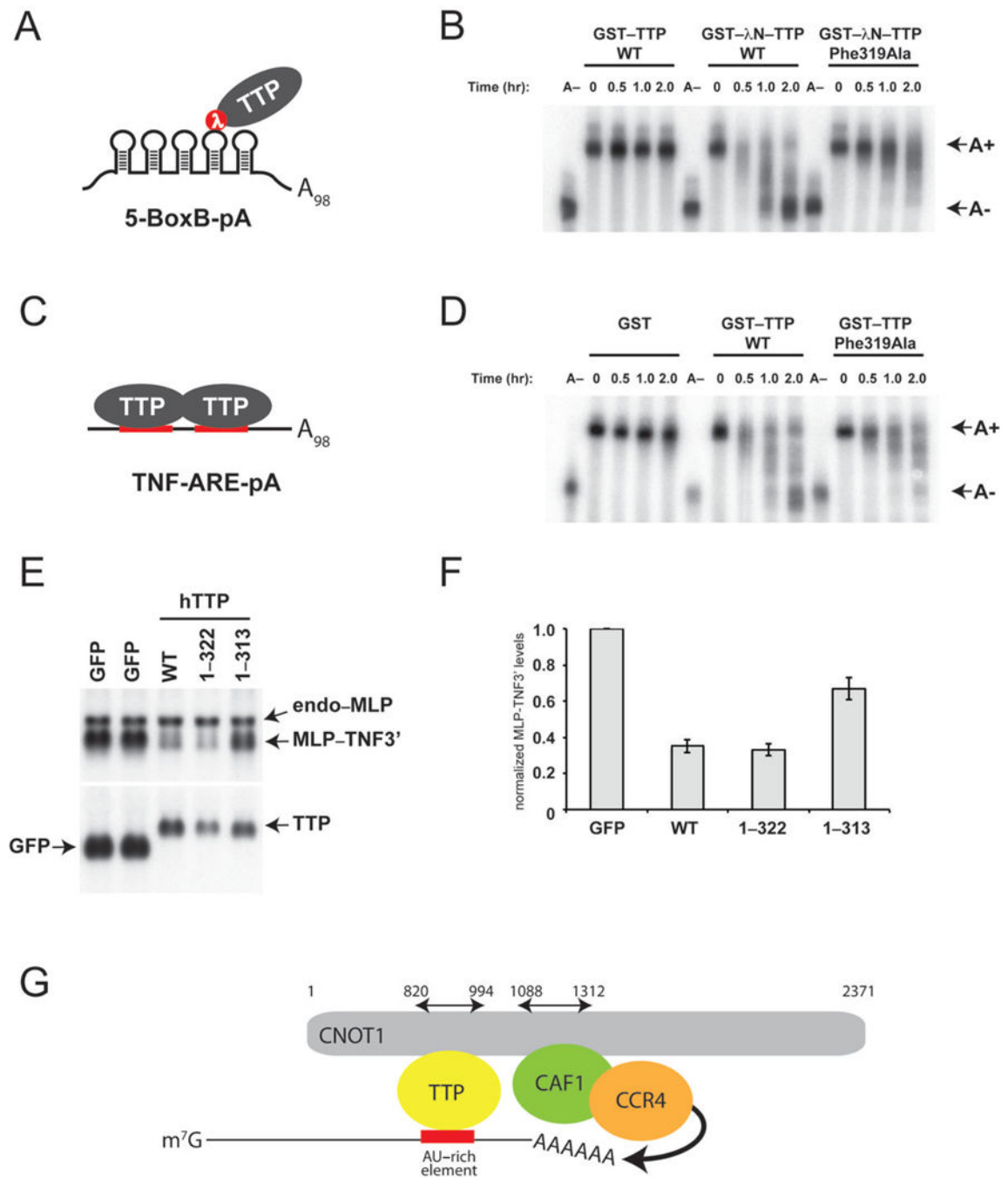


**Figure 4.** Disruption of the TPP-CNOT1 interaction impairs mRNA deadenylation *in vitro* and mRNA stability *in vivo*. **(A)** Schematic depiction of GST-λNHA-TPP tethered to 5-BoxB-pA RNA. **(B)** 5-BoxB-pA RNA deadenylation in Krebs extract in the presence of recombinant wild-type GST-TTP, or wild-type or mutant (Phe319Ala) GST-λNHA-tagged TPP. A(-) RNA was prepared by incubating 5-BoxB-pA with Oligo(dT) and RNase H. Polyadenylated and deadenylated mRNAs are marked on the right of the figure. **(C)** Schematic depiction of TPP associated with TNF-ARE-pA RNA. **(D)** TNF-ARE-pA RNA

deadenylation in Krebs extract in the presence of recombinant GST, or wild-type or mutant (Phe319Ala) GST-tagged TTP. A(-) RNA was prepared by incubating TNF-ARE-pA with Oligo(dT) and RNase H. Polyadenylated and deadenylated mRNAs are marked on the right of the figure. (E) HEK-293 cells were co-transfected with the reporter construct pMLP-TNF3' and DNA encoding GFP or TTP protein constructs. Total cellular RNA was harvested and subjected to electrophoresis and Northern blotting. In the upper panel, the Northern blot was probed with a <sup>32</sup>P-labeled MLP probe; in the lower panel, the blot was probed with a <sup>32</sup>P-labeled TTP probe. In the upper panel, the endogenous MLP mRNA (endo-MLP) the reporter MLP-TNF3' species are indicated by arrowheads. In the lower panel, the expression levels of transcripts for GFP alone and GFP-TTP are indicated. (F) MLP-TNF3' RNA levels (Figure 4C), normalized to GFP, in the presence of GFP, TTP WT, TTP 1-322 and TTP 1-313. Mean values ±s.e. from seven independent experiments are shown. (G) Model for structural organization of mRNA-bound TTP in complex with CNOT1 and CAF1 and CCR4 deadenylases. The cartoon summarizes structural data reported in this manuscript, combined with data from crystal structures of yeast<sup>20</sup> and human<sup>21</sup> NOT1 proteins in complex with CAF1 and CCR4 deadenylases. TTP and CAF1 binding domains in CNOT1 (820-999 and 1088-1312, respectively) refer to coordinates of human CNOT1 isoform c. Other CCR4-NOT subunits (i.e. CNOT2, 3, 9 and 10) are not shown.

**Table 1**

Data collection and refinement statistics (molecular replacement)

<b>4J8S</b>	
<b>Data collection</b>	
X-ray source	Rotating Cu anode
Wavelength (Å)	1.5418
Resolution (Å)	30-1.55(1.61–1.55)
Space group	<i>P</i> 23
Cell parameters (Å, °)	a=b=c=80.07, α=β=γ=90.00
Molecules per ASU	1
Mosaicity (°)	0.45
No. reflections	57193
Redundancy	11.6(3.5)
<i>I</i> /σ( <i>I</i> )	28.8(2.4)
Completeness (%)	99.0(90.2)
$R_{\text{sym}}^{\dagger}$	0.065(0.45)
$R_{\text{work}}/R_{\text{free}}$	16.1/18.3
<b>Refinement</b>	
Number of atoms, all	1886
Protein	1645
Water	241
R.m.s deviations	
Bond lengths (Å)	0.012
Bond angles (°)	1.313
B-factors (Å <sup>2</sup> ), all	19.75
Protein	18.06
Water	31.23
$R_{\text{work}}/R_{\text{free}}$	16.1/18.3